

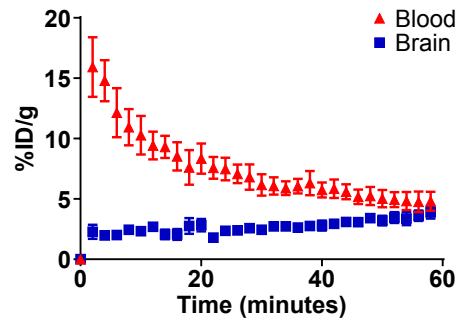
Supplemental information

¹⁸F-FAC PET visualizes brain-infiltrating leukocytes in a mouse model of multiple sclerosis

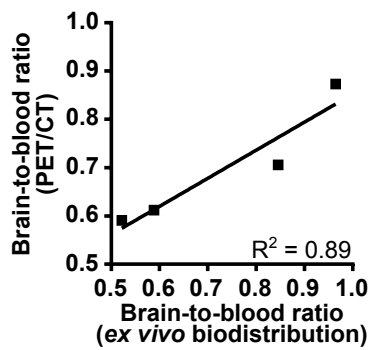
Bao Ying Chen^{1,2}, Chiara Ghezzi^{1,2}, Brendon Villegas³, Andrew

Quon^{1,4}, Caius G. Radu^{1,4}, Owen N. Witte^{1,5,6}, Peter M. Clark^{1,2,5}

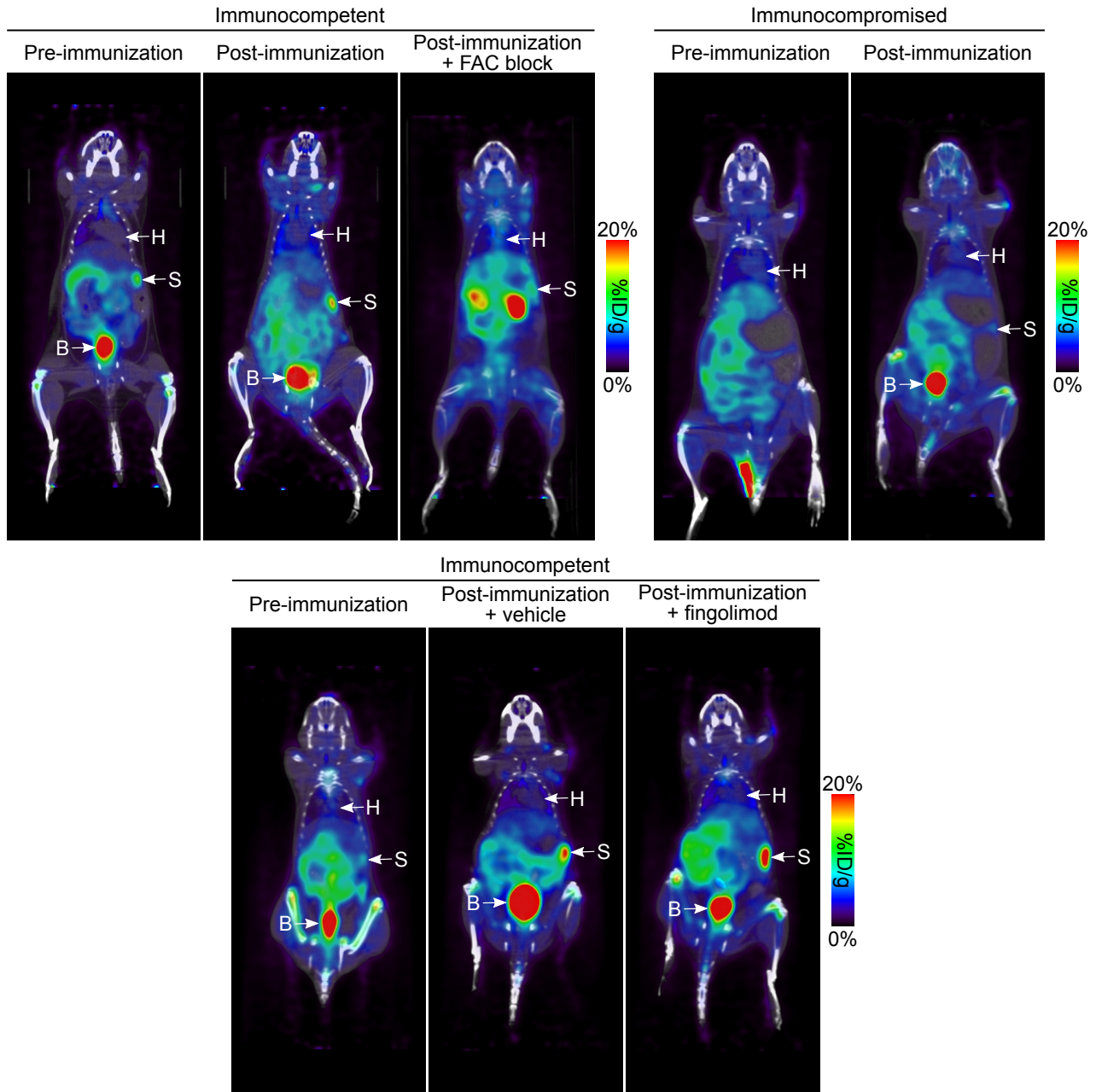
¹ Department of Molecular and Medical Pharmacology, ² Crump Institute for Molecular Imaging, ³ Department of Pulmonary and Critical Care Medicine, ⁴ Ahmanson Translational Imaging Division, ⁵ Eli and Edythe Broad Center of Regenerative Medicine and Stem Cell Research, ⁶ Department of Microbiology, Immunology, and Molecular Genetics, University of California, Los Angeles, CA 90095.



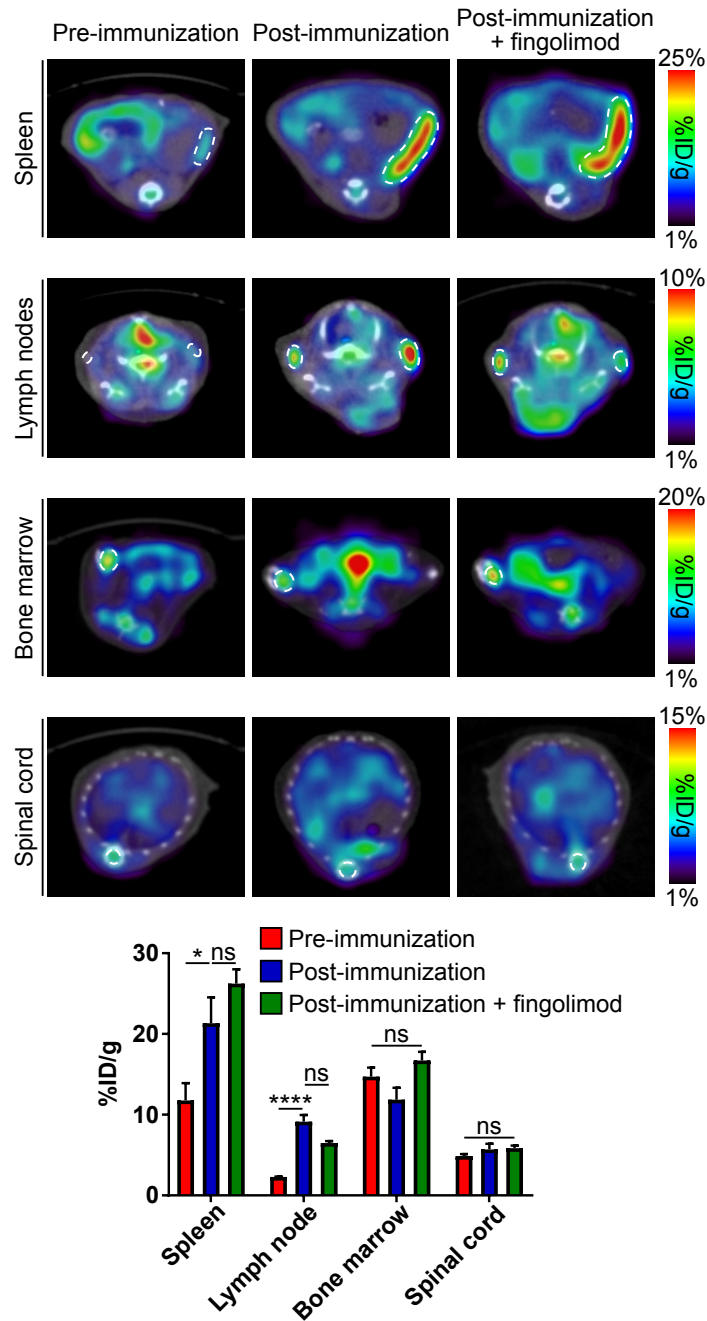
Supplemental Figure 1. Time-activity curves of ^{18}F -FAC accumulation in the blood and brains of healthy mice. $n=5$.



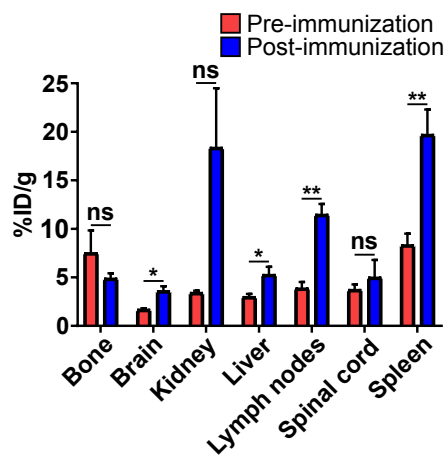
Supplemental Figure 2. Brain-to-blood ratios of ^{18}F -FAC in healthy mice, as measured from the PET/CT images and *ex vivo* biodistribution studies. $n=4$.



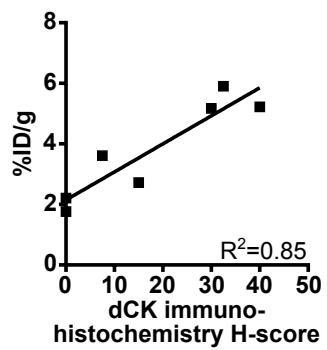
Supplemental Figure 3. ^{18}F -FAC accumulation in immunocompetent and immunocompromised mice pre- and post-immunization, and co-injected with non-radiolabeled FAC (FAC block) or treated with vehicle or fingolimod. H = heart, S = spleen, B = bladder.



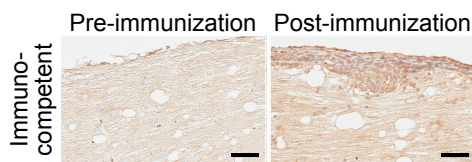
Supplemental Figure 4. ^{18}F -FAC PET can be used to monitor peripheral immune activation at specific locations throughout the body in EAE mice and following treatment with an immunomodulatory drug. Representative transverse ^{18}F -FAC PET/CT images of immunocompetent mice pre-immunization, post-immunization, and post-immunization and treated with fingolimod. Spleen, lymph nodes, bone marrow, and spinal cord encircled in a white dotted line (top). Quantification (bottom). Pre-immunization and post-immunization: $n=7$; post-immunization and treated with fingolimod: $n=3$. *: $P<0.05$; ****: $P<0.0001$, ns: not significant.



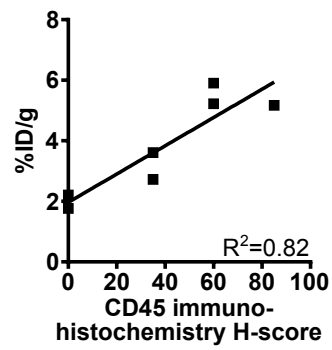
Supplemental Figure 5. ^{18}F -FAC biodistribution, measured *ex vivo* in organs from immunocompetent mice pre- and post-immunization. $n=4$ except for spinal cord which is $n=3$. *: $P<0.05$, **: $P<0.01$, ns: not significant.



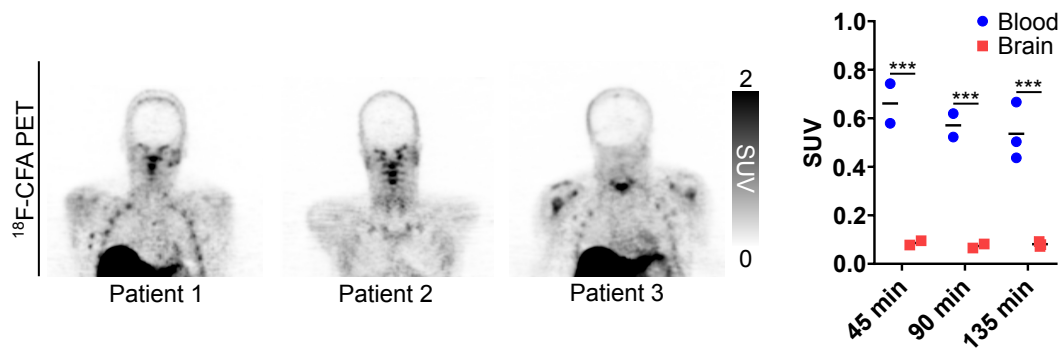
Supplemental Figure 6. dCK immunostaining (as measured by an immunohistochemistry H-score) and ^{18}F -FAC accumulation in the brains of immunocompetent mice. $n=7$.



Supplemental Figure 7. dCK immunostaining of spinal cord tissue sections from immunocompetent mice pre- and post-immunization. 40x magnification images. Scale bars: 50 microns. Representative images of $n=2$.



Supplemental Figure 8. CD45 immunostaining (as measured by an immunohistochemistry H-score) and ^{18}F -FAC accumulation in the brains of immunocompetent mice. $n=7$.



Supplemental Figure 9. $^{18}\text{F-CFA}$ does not readily cross the blood-brain barrier in healthy human subjects. Representative coronal PET images of healthy volunteers injected with $^{18}\text{F-CFA}$ at 135 min post-tracer injection (*left*). Blood and brain $^{18}\text{F-CFA}$ accumulation, quantified from the PET images of healthy volunteers (*right*). The PET scans analyzed here are the same as those reported in Ref. 25. 45 and 90 min time point: $n=2$; 135 min time point: $n=3$. ***: $P<0.001$.